Conceptual Design of a Flight Validation Mission for a Hypervelocity Asteroid Intercept Vehicle

Brent W. Barbee[a,1,*], Bong Wie[b,2], Mark Steiner[c,3], Kenneth Getzandanner[a,1]

[a]*NASA/GSFC, Code 595, 8800 Greenbelt Road, Greenbelt, MD, 20771, USA, 301.286.1837*
[b]*Iowa State University, 2271 Howe Hall, Room 2325, Ames, IA 50011-2271, USA*
[c]*NASA/GSFC, Code 592, 8800 Greenbelt Road, Greenbelt, MD, 20771, USA*

Abstract

Near-Earth Objects (NEOs) are asteroids and comets whose orbits approach or cross Earth's orbit. NEOs have collided with our planet in the past, sometimes to devastating effect, and continue to do so today. Collisions with NEOs large enough to do significant damage to the ground are fortunately infrequent, but such events can occur at any time and we therefore need to develop and validate the techniques and technologies necessary to prevent the Earth impact of an incoming NEO. In this paper we provide background on the hazard posed to Earth by NEOs and present the results of a recent study performed by the NASA/Goddard Space Flight Center's Mission Design Lab (MDL) in collaboration with Iowa State University's Asteroid Deflection Research Center (ADRC) to design a flight validation mission for a Hypervelocity Asteroid Intercept Vehicle (HAIV) as part of a Phase 2 NASA Innovative Advanced Concepts (NIAC) research project. The HAIV is a two-body vehicle consisting of a leading kinetic impactor and trailing follower carrying a Nuclear Explosive Device (NED) payload. The HAIV detonates the NED inside the crater in the NEO's surface created by the lead kinetic impactor portion of the vehicle, effecting a powerful subsurface detonation to disrupt the NEO. For the flight validation mission, only a simple mass proxy for the NED is carried in the HAIV. Ongoing and future research topics are discussed following the presentation of the detailed flight validation mission design results produced in the MDL.

Keywords: Asteroid mitigation, mission design, hypervelocity impact, flight validation, planetary defense

1. Introduction

Earth has a well-documented history of impact by asteroids and comets that were sufficiently energetic, in terms of mass and impact velocity, to cause signficant damage ranging from local or regional devastation to mass extinctions. Such asteroids and comets whose orbits approach or cross Earth's orbit are designated near-Earth objects (NEOs). At present there are at least tens of thousands of undiscovered NEOs larger than 100 m in diameter. Any of these may be found to be on a collision course with Earth and therefore require a planetary defense mission to deflect or destroy it prior to Earth impact. Our current NEO detection and tracking programs are making significant strides in discovering these NEOs and monitoring their orbits for future Earth impacts to provide advance warning of any threats. We have also sent a number of scientific missions to asteroids and comets that provide heritage on which future planetary defense missions can build. However, no planetary defense flight validation missions have been deployed and the capability to deflect or destroy a threatening NEO therefore remains unproven.

Some of the key factors in designing planetary defense systems include the size of the incoming NEO and the amount of warning time. The size of the NEO determines how much damage it would cause and places limits on our response options, while the warning time further constrains our options for dealing with the NEO.

Opportunities to rendezvous with NEOs at a reasonable propellant mass cost tend to occur infrequently, so for scenarios in which the NEO impact event is known less than 10 years in advance, the most viable option will likely be hypervelocity intercept in which our mitigation system is delivered to the NEO at high relative velocity because the propellant cost to match the NEO's orbital velocity would be prohibitive. Although larger NEOs are capable of causing more damage than smaller ones, the small NEOs are far more numerous and thus a small NEO impact scenario is more likely within any given time frame, all else being equal. Unfortunately, small NEOs are fainter in the night sky and therefore harder to discover and track with ground-based telescopes in advance of when they would collide with Earth. Additionally, small NEOs are more difficult for a spacecraft to target (i.e., acquire optically with onboard cameras), especially at high relative velocity. Thus the most challenging NEO mitigation scenario involves a small NEO with relatively short warning time, requiring a hypervelocity intercept for deflection or destruction of the NEO. A spacecraft system capable of reliably handling that scenario would of course be able to handle less stressing cases, i.e., more warning time, lower intercept velocities, and larger NEOs.

Work was recently performed towards the design of such a spacecraft system by the Asteroid Deflection Research Center (ADRC) in the Department of Aerospace Engineering at Iowa State University and the Mission Design Laboratory (MDL) of NASA Goddard Space Flight Center's Integrated Design Center (IDC). The goal of this work is to assess the technical feasibility of reliably performing hypervelocity interception of a 50 m diameter NEO and design a spacecraft and mission architecture for flight validation of the system. This research was funded by and in support of the recently awarded NASA Innovative Advanced Concepts (NIAC) Phase II study entitled "An Innovative Solution to NASA's NEO Impact Threat Mitigation Grand Challenge and Flight Validation Mission Architecture Development." The goals of this research project include designing a two-body Hypervelocity Asteroid Intercept Vehicle (HAIV) to deliver a kinetic impactor to the target NEO that will excavate a shallow crater in which the second portion of the spacecraft will detonate a Nuclear Explosive Device (NED) immediately thereafter to effect a powerful subsurface detonation capable of disrupting the NEO; subsurface detonations are believed to be on the order of 20 times more effective at disrupting a NEO than detonations on or above the NEO's surface. The flight validation mission will carry an inert dummy payload with the same mass properties as a NED. Flight validation of this system is crucial because any NEO mitigation system must be thoroughly flight tested before it can be relied upon during a true emergency, and no such flight validations have been performed.

In this paper we first review the current status of the NEO impact hazard and establish the need for planetary defense flight validation missions. We then provide a detailed overview and summary of the HAIV concept and MDL study results including: the selected notional target NEO for the flight validation mission; the conceptual configuration of the HAIV and its subsystems; guidance, navigation, and control (GNC) analysis results regarding the ability of the HAIV to reliably target and intercept small (50 m) NEOs at hypervelocity (typically > 5–10 km/s); the mission scenario and trajectory design for the notional flight validation mission to a selected candidate target NEO chosen for safety and mission affordability; and important research topics identified by the MDL study to be addressed in ongoing research.

2. The NEO Impact Hazard

Recent decades have seen considerable improvement in our understanding of the NEO population and the hazard that NEOs pose to Earth. Ground-based survey programs, such as LINEAR, the Catalina Sky Survey, and the emerging Pan-STARRS and LSST systems, have discovered many near-Earth asteroids (NEAs) and near-Earth comets (NECs). Automated computer systems, such as the Sentry system at the NASA Jet Propulsion Laboratory (JPL) and the NEODyS system at the University of Pisa, continually monitor the known NEO population to determine whether any NEOs have a non-zero probability of collision with Earth. Ground-based discovery and tracking, combined with automated impact probability monitoring, will afford us advance warning of an Earth-impacting NEO if its heliocentric orbit geometry and phasing relative to Earth allow it to be detected by ground-based telescopes prior to the time of Earth impact.

As of March 9th, 2013, 9,667 NEAs and 93 NECs have been discovered[4], yielding a total of 9,760 known NEOs. 1,380 of these are classified as Potentially Hazardous Asteroids (PHAs), meaning that their Earth Minimum Orbit Intersection Distances (MOIDs) are ≤ 0.05 AU (approximately 7,480,000 km) and their estimated diameters are ≥ 150 m.

Earth is typically struck by very small NEOs (on the order of one to several meters in diameter) multiple times each year. These objects typically burn up or explode high in the upper atmosphere and thus do not generally pose a direct threat to the Earth's surface. One such collision event occurred in October of 2008 when a small asteroid,

---

[4] `http://neo.jpl.nasa.gov/stats/`, accessed 2013-03-09

perhaps 2 to 5 m in diameter, designated 2008 TC$_3$ was discovered approximately 20 hours before it struck Earth. The asteroid released approximately 2 kilotons of energy when it exploded high above northern Sudan. Researchers were able to retrieve nearly 600 fragments of the object several months later. Impacts by these very small NEOs (i.e., high altitude explosions) are monitored via worldwide infrasound sensors to distinguish them from weapons testing or deployment.

NEOs somewhat larger than 2008 TC$_3$, up to a few tens of meters in diameter, pass within lunar distance of the Earth every few weeks. However, our telescopes do not always detect these small NEAs because their small size makes them relatively faint in the night sky. In some cases they may approach from the sunward direction and hence do not appear in our night sky at all. A famous upcoming close approach is that of the NEO designated 99942 Apophis (2004 MN4). This 330 m diameter object will closely approach Earth in April of 2029 at a distance of approximately 32,000 km. If Apophis were to strike Earth it would release approximately 750 megatons of energy, far more powerful than the largest nuclear weapons ever tested.

Two significant NEO events occurred recently on February 15th, 2013. The first event of the day was the impact of an approximately 17 to 20 m NEO over the city of Cheylabinsk in Russia. The 440 kiloton explosion at an altitude of 23 km shattered many windows, damaged some buildings, and injured at least 1400 people in the process. This was the most energetic such event recorded since the Tunguska event of 1908, in which a NEO estimated to have been at least several tens of meters in diameter exploded several kilometers above the ground near the Podkamennaya Tunguska River in what is now Russia and devastated an area approximately the size of Washington, DC. Only 16 hours after the Cheylabinsk event, the 40 m NEA 2012 DA$_{14}$ reached its point of closest approach to Earth at an altitude of approximately 27,600 km. This is the closest approach on record by a NEO of that size. Despite the fact that these two events occurred only hours apart, there is no relationship between the 2012 DA$_{14}$ close approach and the Cheylabinsk event[5].

The surface of our moon is clearly covered in craters from past impacts and our own planet also bears the scars of celestial bombardment, though they are largely obscured by weathering, vegetation, and the fact that the majority of Earth's surface is covered by water. Nevertheless, 184 confirmed impact structures[6] have been discovered on Earth thus far, many of which are larger than 20 km in diameter. One of the largest and most famous craters is the Chicxulub crater in the Yucatan peninsula, which was created approximately 65 million years ago by the impact of a 9 to 19 km sized asteroid or comet. That impact caused the Cretaceous-Paleogene (K-Pg) extinction event during which the dinosaurs were made extinct, along with most other species living at the time. One of the most recognizable Earth impact structures is the Barringer Meteor crater, shown in Figure 1, which was created around 50,000 years ago when a nickel-iron meteorite approximately 50 m in size struck the ground about 55 km east of Flagstaff, Arizona. This impact produced a 2.5 megaton explosion that created a crater 1.2 km wide and 170 m deep, killed all life within a 4 km radius instantly, leveled everything within a 22 km radius, and generated hurricane-force winds out to a radius of 40 km.

Figure 1: The Barringer meteor crater in Arizona.

While our own planet and moon show ample evidence of past impact events, we have also observed three large-scale collisions of comets or asteroids with the planet Jupiter. Between July 16th and 22nd in 1994 more than 20 pieces of the comet Shoemaker-Levy 9 struck Jupiter, and our observations of that event constituted the first time we had ever directly observed such a collision. A Hubble Space Telescope image of this event is presented in Figure 2. Jupiter has been hit by smaller asteroids or comets twice more that we are aware of, on July 19th, 2009, and June 3rd, 2010. More recently, a retrograde Oort cloud comet designated C/2013 A1 (Siding Spring)

---

[5] http://neo.jpl.nasa.gov/news/fireball_130301.html, accessed 2013-03-10
[6] http://www.passc.net/EarthImpactDatabase/index.html, accessed 2013-03-09
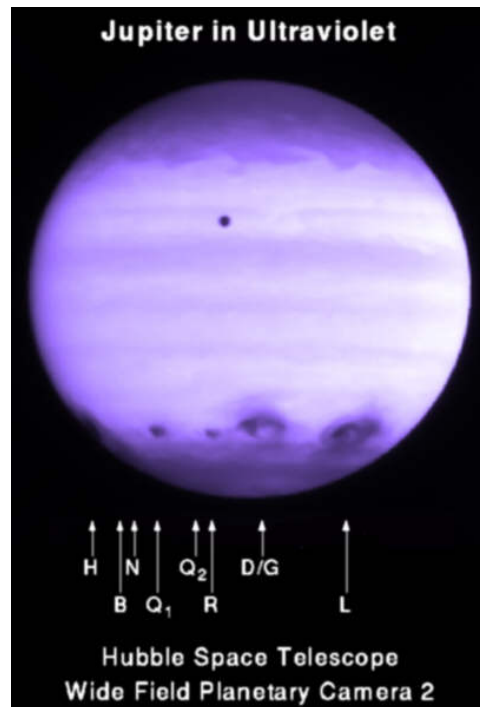
Figure 2: Collision scars on Jupiter after the 1994 impact of comet Shoemaker-Levy 9.

has been discovered that will pass extremely close to Mars on October 19th, 2014 at a distance less than 300,000 km (50,000 km is the current best estimate)[7]. The uncertainty in our knowledge of the comet's trajectory leaves open the possibility that this comet will collide with Mars; a Mars collision cannot be confirmed or excluded until additional observations of the comet are obtained to improve our knowlege of its trajectory. This comet will pass or collide with Mars at a relative velocity of approximately 56 km/s and is estimated to be 3 to 50 km in size. As such, if this comet does impact Mars it will release a tremendous amount of energy and create a crater tens or hundreds of kilometers in diameter.

Statistical models of the total NEO population allow us to estimate how many NEOs remain to be discovered, and recent data from the NEOWISE mission has yielded an updated estimate of the size of the NEO population. The estimated population of NEOs > 1 km in diameter is nearly 1000; just over 90% of these have been discovered and determined to not pose a threat to Earth. However, there are an estimated 16,300 NEOs with diameters between 100 and 1000 m yet to be discovered. Thus far approximately 3,000 NEOs with diameters < 100 m have been discovered and there may well be hundreds of thousands, if not millions, of NEOs in this size category yet to be discovered.

Thus there are many thousands of undiscovered NEOs lurking in our inner solar system large enough to cause significant damage, and we must be prepared to deflect or destroy any that are found to be on a collision course with our planet. NEO impacts are aperiodic events from our limited perspective and they can therefore occur at any time with little or no warning. Our nation's space program has wisely invested in discovery, tracking, and impact risk monitoring efforts, and the time has now come to expand those efforts and begin investing in the spacecraft systems and technologies that will be required to successfully deflect or destroy an incoming NEO. Advance warning of the impact is not actionable unless we have also adequately prepared ourselves to respond effectively to the threat.

3. The Need for Planetary Defense Flight Validation Missions

At present there have been no flight missions to validate planetary defense techniques or technologies. However, between 1986 and 2011, a total of 11 science spacecraft have performed flybys of 6 comets and 7 asteroids, and rendezvoused with 3 asteroids. The first of these were the Vega 1, Vega 2, and Giotto spacecraft, all of which performed flybys of comet 1P/Halley in 1986. The Galileo spacecraft closely approached two asteroids: 951 Gaspra in 1991 and 243 Ida in 1993. Meanwhile, Giotto performed a flyby of comet 26P/Grigg-Skjellerup in

---

[7]http://neo.jpl.nasa.gov/news/news179.html, accessed 2013-03-09

1992. In 1997, the NEAR-Shoemaker spacecraft flew past the asteroid 253 Mathilde on the way to the asteroid 433 Eros, where the spacecraft entered a captured orbit and performed an extended scientific survey. During the same time frame, the Deep Space 1 spacecraft performed a flyby of asteroid 9969 Braille in 1999 and comet 19P/Borrelly in 2001. Following this, the Stardust spacecraft flew by asteroid 5535 Annefrank in 2002 and comet 81P/Wild in 2004. With the exception of NEAR-Shoemaker, all of these missions only flew past the asteroids or comets at distances of several hundred to several thousand kilometers. This changed in 2005 when the Deep Impact spacecraft successfully deployed an impactor to collide with comet 9P/Tempel, creating the spectacular display seen in Figure 3. During the same year, the Hayabusa/MUSES-C spacecraft rendezvoused with asteroid

Figure 3: Collision of the impactor with comet Tempel 1 during the 2005 Deep Impact mission.

25143 Itokawa and eventually returned tiny grains of asteroid material to Earth. An image of Itokawa obtained during the mission is shown in Figure 4. The Rosetta spacecraft flew past the asteroids 2867 Steins in 2008 and

Figure 4: Asteroid Itokawa as seen during JAXA's Hayabusa/MUSESC mission in 2005.

21 Lutetia in 2010 on its way to a 2014 rendezvous with comet 67P/Churyumov-Gerasimenko. After flying past comet 9P/Tempel in 2005, The Deep Impact spacecraft continued operating in an extended mission and was directed to perform a flyby of comet 103P/Hartley in 2010. Deep Impact may be re-tasked yet again to perform a flyby of a PHA known as 2002 GT during the year 2020. The Dawn mission is currently in orbit around 4 Vesta, the largest known main belt asteroid (now understood to be a proto-planet thanks to data collected by Dawn), and will proceed to rendezvous with the dwarf planet Ceres, also located in the main asteroid belt, during the year 2015. NASA is currently developing the OSIRIS-REx mission, which will launch in the year 2016 to rendezvous with the PHA known as 101955 (1999 RQ_{36}) and return to Earth with samples of the asteroid in 2023. The Japanese space program is currently considering an asteroid sample return mission known as Hayabusa 2, which would launch in 2014 with the goal of returning samples from the PHA known as 162173 (1999 JU_3), and a mission named Hayabusa Mk2 to the dormant comet designated 4015 Wilson-Harrington (1979 VA). Finally,

the European Space Agency (ESA) is currently studying the MarcoPolo-R mission concept, in which samples would be returned from the PHA designated 34184 (2008 EV$_5$). This mission was originally targeting the binary asteroid 175706 (1996 FG$_3$). The aforementioned previous asteroid and comet flybys are summarized in Table 1 with flyby distances and relative velocities for cases where those quantities are known. Table 2 summarizes the aforementioned previous asteroid rendezvous missions, and Table 3 lists planned upcoming asteroid and comet rendezvous missions.

Table 1: Previous flybys of comets and asteroids.

Flyby Date	Spacecraft	Object	Type	Size (km)	Distance (km)	Rel. Vel. (km/s)
1986-03-06	Vega 1	1P/Halley	Comet	15×8	8889	
1986-03-09	Vega 2	1P/Halley	Comet	15×8	8030	
1986-03-14	Giotto	1P/Halley	Comet	15×8	596	
1991-10-29	Galileo	951 Gaspra	MBA	$18.2 \times 10.5 \times 8.9$	1600	8.00
1992-07-10	Giotto	26P/GriggSkjellerup	Comet	2.6	200	
1993-08-28	Galileo	243 Ida	MBA	$53.6 \times 24.0 \times 15.2$	2390	12.40
1997-06-27	NEAR-Shoemaker	253 Mathilde	MBA	$66 \times 48 \times 46$	1212	9.93
1999-07-29	Deep Space 1	9969 Braille	MBA	$2.1 \times 1.0 \times 1.0$	26	
2001-09-21	Deep Space 1	19P/Borrelly	Comet	$8 \times 4 \times 4$	2173	
2002-11-02	STARDUST	5535 Annefrank	MBA	$6.6 \times 5.0 \times 3.4$	3079	
2004-01-02	STARDUST	81P/Wild	Comet	$5.5 \times 4.0 \times 3.3$	237	6.10
2005-07-04	Deep Impact	9P/Tempel	Comet	7.6×4.9	0	10.30
2008-09-05	Rosetta	2867 Steins	MBA	$6.67 \times 5.81 \times 4.47$	800	8.60
2010-07-10	Rosetta	21 Lutetia	MBA	$121 \times 101 \times 75$	3168	15.00
2010-11-04	Deep Impact	103P/Hartley	Comet	2.2×0.5	700	12.31
2011-02-15	STARDUST	9P/Tempel	Comet	7.6×4.9	181	

Table 2: Previous asteroid rendezvous missions.

Rendezvous Date	Spacecraft	Object	Type	Size (km)
2000-02-14	NEAR-Shoemaker	433 Eros	NEA	$34.4 \times 11.2 \times 11.2$
2005-09-12	Hayabusa/MUSES-C	25143 Itokawa	PHA	$0.535 \times 0.294 \times 0.209$
2011-07-16	Dawn	4 Vesta	MBA	$578 \times 560 \times 458$

Table 3: Planned asteroid/comet rendezvouses.

Rendezvous Date	Spacecraft	Object	Type	Size (km)
2014-05	Rosetta	67P/ChuryumovGerasimenko	Comet	4.0
2015-02	Dawn	1 Ceres	MBA	487.3×454.7
2018	Hayabusa 2	162173 (1999 JU$_3$)	PHA	0.98
2018-10	OSIRIS-REx	101955 (1999 RQ$_{36}$)	PHA	0.56
> 2018	Hayabusa Mk2	4015 Wilson-Harrington (1979 VA)	PHA	4.0
> 2022	MarcoPolo-R	34184 (2008 EV$_5$)	PHA	0.45

Each of the aforementioned science missions required at least several years, in some cases 5 to 6 years or more, for mission concept development and spacecraft construction prior to launch. It is also important to note that some of these missions were originally targeting different asteroids or comets than those that were actually visited. This is because the mission development schedules slipped and launch windows for particular asteroids or comets were therefore missed. Additionally, several of these missions experienced hardware or software failures or glitches that compromised the completion of mission objectives. None of those things would be tolerable for a planetary defense mission aimed at deflecting or destroying an incoming NEO, possibly with relatively little advance warning. Thus, while the impressive scientific missions that have been sent to asteroids and comets so far have certainly provided future planetary defense missions with good heritage on which to build, we are clearly not ready to respond reliably to a threatening NEO scenario.

Finally, it is also important to note that most of these missions visited asteroids or comets that range in size from several kilometers to several tens of kilometers. Furthermore, the flyby distances ranged from several tens of kilometers to several thousand kilometers. The sole exception to this is the Deep Impact mission, which succeeded in delivering an impactor to the target. However, the mission was aided by the fact that comet 9P/Tempel, is 7.6 × 4.9 km in size and therefore provided a relatively large target to track and intercept. Consequently, the Deep Impact mission was not intended to be a planetary defense technology flight validation mission. For planetary defense missions requiring NEO intercept, the requirements will be far more stringent: NEO targets with diameters as small as 50 m will have to be reliably tracked and intercepted at hypervelocity, with impact occurring within mere meters of the targeted point on the NEO's surface. This will require significant evolution of the autonomous Guidance, Navigation, and Control (GNC) technology currently available for spacecraft missions to NEOs. Furthermore, none of the potential planetary defense mission payloads to deflect or destroy a NEO have ever been tested on NEOs in the space environment. Significant work is therefore required to appropriately characterize the capabilities of those payloads, particularly the ways in which they physically couple with a NEO to transfer energy or alter momentum, and ensure robust operations during an actual emergency scenario.

When a hazardous NEO on a collision course with Earth is discovered we will not have the luxury of selecting a NEO target suitable for our mission design purposes or changing our choice of target if our development schedule slips. Instead, nature will have selected the target for us, along with whatever challenges are posed by its orbit and physical characteristics. Making preparations now is essential because we will only have one chance to deploy an effective and reliable defense.

4. Overview of the HAIV Mission Concept

The Hypervelocity Asteroid Intercept Vehicle (HAIV) system and mission architecture were initially developed during a NIAC Phase 1 research study [1] and preliminary results prior to the conclusion of that study have also been documented in the technical literature [2, 3]. The HAIV concept blends a kinetic impactor with a Nuclear Explosive Device (NED) delivery system to execute a subsurface detonation with the goal of disrupting the target NEO. While standalone kinetic impactors have been proposed and studied for the purpose of deflecting (rather than disrupting) a NEO, the purpose of the kinetic impactor portion of the HAIV is to create a shallow crater in the surface of the target NEO. The NED carrier portion of the HAIV, which is following immediately behind the leading kinetic impactor portion, flies into the crater and detonates the NED before striking the bottom of the crater. This sequence of events is depicted in Figure 5. The result is a slightly subsurface nuclear detonation
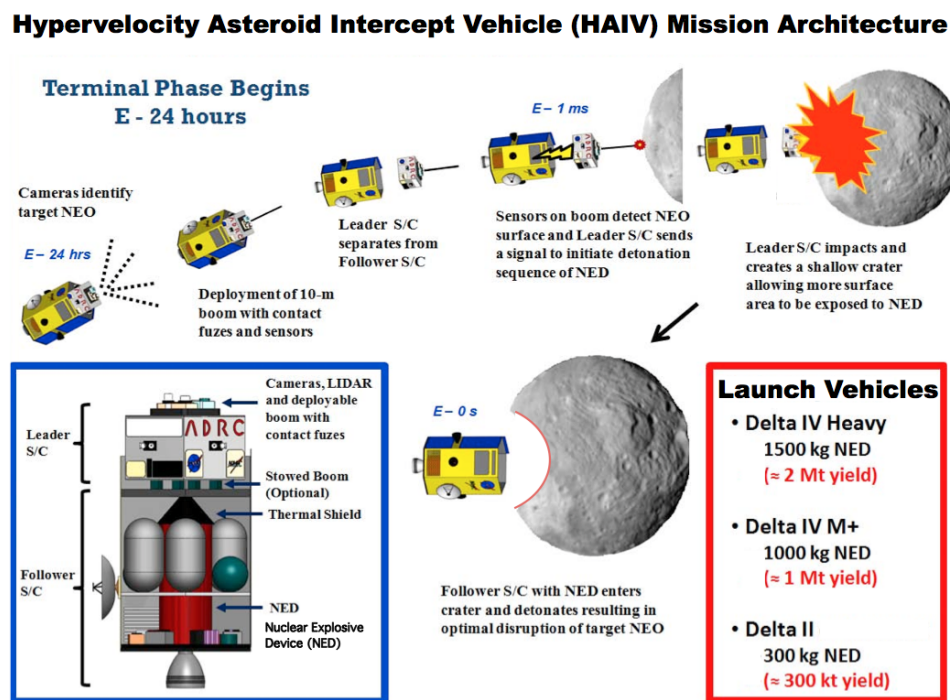

Figure 5: A baseline HAIV and its terminal-phase operational concept [1, 3].

that is approximately 20 times more effective at disrupting the body of the target NEO than a surface or standoff

detonation. Figure 6 shows a simplified 2-D computational modeling and simulation of a penetrated, 70 kiloton nuclear explosion for a 70 m asymmetric reference target body.
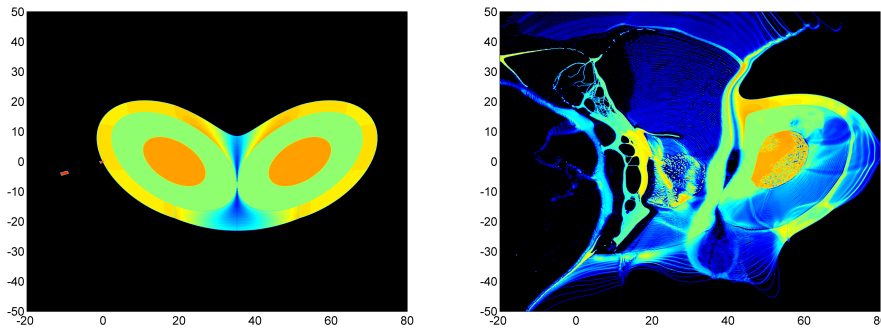

Figure 6: Simulated disruption of a small asymmetrically shaped NEO by a subsurface NED detonation [1, 3].

The enhanced effectiveness of the subsurface detonation reduces the yield (mass) of the NED required to deal with a given NEO, all else being equal, and that improves responsiveness by not over-burdening the launch vehicle. Responsiveness is a key theme here because one of the primary objectives of the HAIV design is to provide a reliable solution for mitigating the threat posed by short warning time (< 10 years of warning) scenarios. In such scenarios the HAIV will need to be launched onto a direct high-energy trajectory to intercept the NEO not long before the NEO would have struck the Earth absent our intervention. It is a consequence of orbital dynamics that such intercept trajectories tend to have high relative velocities between the HAIV and NEO at the time of intercept. These relative velocities will typically be in the hypervelocity regime (> 5 km/s), and a prohibitively large mass of propellant would be required to nullify that relative velocity for rendezvous with the NEO. This motivates our goal of designing a robust and precise hypervelocity intercept platform. Furthermore, we turn the hypervelocity nature of the intercept to our advantage by using the leading kinetic impactor portion of the HAIV to excavate the shallow crater for the subsequent subsurface NED detonation. The primary challenges include developing robust and precise GNC systems capable of reliably performing hypervelocity intercept of NEOs and creating highly responsive and reliable hypervelocity impact detection and NED detonation systems.

The Phase 2 NIAC research is focused on further design of the system and development of a flight validation mission concept to demonstrate the capability to handle short warning time NEO impact scenarios involving the more numerous smaller NEOs in the 50–100 m size category. Phase 2 tasks include three-dimensional hyper-velocity impact and nuclear explosion modeling and simulation using next-generation Graphics Processing Unit (GPU) computers; HAIV design trades, including concepts for leader/follower vehicle separation such as a 10–20 m deployable boom versus free-flying (i.e., not physically connected) vehicles; study of various options for hyper-velocity impact detectors/sensors; and design of GNC algorithms to enable robust and reliable precision impact with a small (50–100 m) irregularly shaped rotating NEO using advanced optical navigation and guidance logic. Our Phase 2 research will ultimately lead to the development of a proposal for a flight validation mission of the HAIV system, ideally within a mission cost cap of approximately \$500M. We are also exploring the possible benefits of conducting ground experiments using scaled HAIV models instrumented with candidate hypervelocity impact sensors/detectors. One of the first steps in our Phase 2 research program was the commissioning of a study to begin developing the HAIV flight validation mission concept in the Mission Design Lab (MDL) at the NASA Goddard Space Flight Center (GSFC). In subsequent sections herein we describe the selection of a notional target NEO for the conceptual flight validation mission and the MDL study results for the flight validation mission design.

5. Notional Flight Validation Mission Target Selection

The ADRC has been developing trajectory scan techniques for identifying the best NEO targets for various flight validation mission concepts [4, 5]. Those techniques were further developed to perform trajectory scans for thousands of NEOs to identify the best choice of target NEO for the notional flight validation mission scenario that we would then study in the MDL. One of our primary criteria for the mission is safety—we do not want the flight validation mission to pose any risk of turning a harmless NEO into an Earth impactor. For that reason we restrict our candidate target set to only include NEOs from the Amor and Atira groups, whose orbits are entirely exterior or interior to Earth's orbit, respectively, as shown in Figure 7.

Amors

Earth-approaching NEAs with orbits
exterior to Earth's but interior to Mars'
(named after asteroid (1221) Amor)
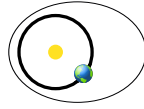
$a > 1.0$ AU
1.017 AU $< q < 1.3$ AU

Apollos

Earth-crossing NEAs with semi-major
axes larger than Earth's
(named after asteroid (1862) Apollo)

$a > 1.0$ AU
$q < 1.017$ AU

Atens

Earth-crossing NEAs with semi-major
axes smaller than Earth's
(named after asteroid (2062) Aten)

$a < 1.0$ AU
$Q > 0.983$ AU

Atiras

NEAs whose orbits are contained
entirely within the orbit of the Earth
(named after asteroid (163693) Atira)

$a < 1.0$ AU
$Q < 0.983$ AU

(q = perihelion distance, Q = aphelion distance, a = semi-major axis)

Figure 7: NEO groups according to orbit type.

Our ultimate goal is to develop a robust capability to perform hypervelocity intercept of NEOs as small as 50 m in size, but we decided that a somewhat larger target would be more appropriate for the very first flight validation mission. Figure 8 depicts the trade space that we considered. As indicated in Figure 8, we decided that
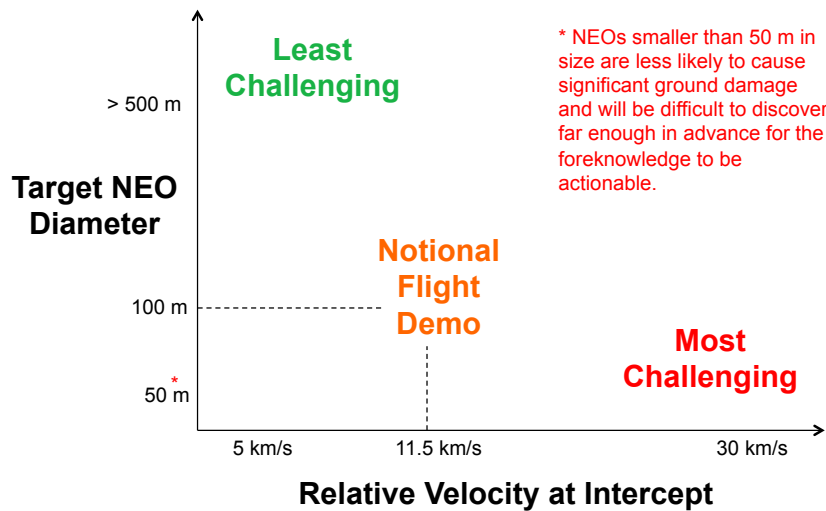
Figure 8: Depiction of the trade space for selecting a target NEO for a flight validation mission.

intercepting an approximately 100 m size NEO at 11.5 km/s provides a practical scenario for the very first flight validation mission, sufficiently challenging to test the capability we want to prove, but not so challenging as to be unreasonable for the first effort. We therefore filtered our list of candidate targets to identify those with estimated diameters around 100 m.

Another consideration in our target search is how well the orbit of the NEO is known. If there is too much uncertainty in our knowledge of the NEO's orbit it may not be possible to guide the HAIV to a precision intercept with the NEO. The quality of NEO orbit knowledge is usually expressed by the Orbit Condition Code (OCC)[8], which is an integer scale describing the amount of along-track uncertainty in the NEO orbit knowledge. The size, shape, and orientation of NEO orbits are generally easier to estimate than the position of the NEO along its orbital path, and the location of the NEO on its orbit is therefore usually the least well known aspect of the NEO's orbit.

---

[8]OCC is also known as the Minor Planet Center (MPC) "U" parameter, for which the technical details are provided at `http://www.minorplanetcenter.net/iau/info/UValue.html`, accessed 2013-03-10.

The OCC scale ranges from 0 (a very well known orbit) to 9 (very poor orbit knowledge), and NEOs with OCC > 5 are generally considered "lost" for the purposes of locating them in the sky during future observing opportunities. We thus applied a filter of OCC ≤ 5 to our NEO target search.

In summary, our trajectory scans were applied to Amor and Atira NEOs with estimated diameter near 100 m and OCC ≤ 5. The trajectory scan constraints included Earth departure characteristic energy $C_3 \leq 12.5$ km^2/s^2, Earth departure date between 2018 and 2020, Sun-Spacecraft-Earth (SSE) angle at the time of intercept > 3°, and phase angle at intercept ≤ 90°. The SSE angle is measured between the vector that points from the spacecraft to the Sun and the vector that points from the spacecraft to the Earth. If the SSE angle is too small then the Sun may interfere with communications between the spacecraft and Earth, and we require a good communications link with the spacecraft, especially at the time of NEO intercept, in order to collect the telemetry needed to confirm the success of the experiment. The phase angle at intercept is measured between the velocity vector of the spacecraft relative to the NEO and the heliocentric position vector of the NEO at the time of intercept. A phase angle of zero places the spacecraft directly between the Sun and the NEO at the time of intercept, while a phase angle of 90° means that the spacecraft approaches the NEO orthogonal to the NEO-Sun line. Designing the trajectory so that a small value of the phase angle obtains provides a situation in which the Sun is naturally illuminating the full face of the NEO, or nearly so, from the spacecraft's perspective during terminal approach, which is highly advantageous for optical acquisition of the NEO with the spacecraft's onboard cameras and especially important for small NEOs that are optically faint even under such ideal circumstances.

After analyzing the trajectory scan results we settled on the NEA designated 2006 CL$_9$ as the notional target for our conceptual flight validation mission. The physical and orbit properties[9] of 2006 CL$_9$ are presented in Table 4. The orbital elements for the NEO presented in Table 4 are heliocentric ecliptic J2000 orbital elements at epoch JD 2456400.5 (2013-04-18.0) TDB (JPL Orbit ID 26).

Table 4: Physical and orbital properties of notional flight validation mission target 2006 CL$_9$.

Property	Value
Absolute magnitude, H	22.73
Estimated diameter w/ $p = 0.13$	104 m
Estimated diameter w/ $p = 0.25$	75 m
Rotation period (hours)	0.145 ± 30%
Semi-major axis, a (AU)	1.34616
Eccentricity, e	0.23675
Inclination, i	2.93551°
Longitude of Ascending Node, Ω	139.313°
Argument of Perihelion, ω	9.94912°
Mean Anomaly at Epoch, M	209.664°
OCC	5
Earth MOID (AU)	0.03978

Another factor in our selection of 2006 CL$_9$ is that while its OCC of 5 would present navigation challenges for our mission, there may be opportunities to gather more ground-based observations of this NEO within the next couple of years, which may improve our knowledge of its orbit and thus reduce the OCC. It happens that this NEO meets the criteria for NASA's Near-Earth Object Human Space Flight Accessible Targets Study (NHATS)[10] [6] and the next upcoming observing opportunity is among the NHATS data published for the NEO[11]. These data show that the NEO should be optically observable from Earth again in June of 2014 with a peak visual magnitude of 22.9.

Note that two estimated diameter values for 2006 CL$_9$ are presented in Table 4 based on the parameter p, which is the geometric albedo of the NEO (a measure of how optically reflective its surface is). The albedos of NEOs vary widely and are very difficult to ascertain from ground based observations. This leads to significant uncertainty in the physical size of most known NEOs. The problem can be summarized thusly: small shiny objects can have the same brightness in the sky as large dull objects. The brightness of the NEOs, expressed by the absolute magnitude, H, is much better constrained (because it is directly observed) than albedo. We must assume an albedo for our NEO in order to compute the estimated diameter[12] and as shown in Table 4 we used albedo values of 0.13 and

---

[9]http://ssd.jpl.nasa.gov/sbdb.cgi?sstr=2006CL9, accessed 2013-03-10.

[10]http://neo.jpl.nasa.gov/nhats/

[11]http://neo.jpl.nasa.gov/cgi-bin/nhats?sstr=2006CL9&dv=12&dur=450&stay=8&launch=2015-2040

[12]http://www.physics.sfasu.edu/astro/asteroids/sizemagnitude.html, accessed 2013-03-10.

0.25. Those are reasonable values for NEO albedo and yield an estimated size between 75 and 105 m, which is near the 100 m value we desire. All that being said, note that the NHATS data for this NEO show an estimated diameter range of 49 to 221 m, based on albedos of 0.6 and 0.03, respectively, and so it is possible that this NEO is anywhere from half the size to double the size we have estimated with an albedo of 0.13.

The mission trajectory selected for 2006 CL$_9$ is summarized in Table 5. The baseline trajectory design is based on patched conics with Lambert targeting applied to high-fidelity ephemerides for the Earth and NEO, and therefore no determinstic Δv is required on the part of the spacecraft in this initial trajectory design. However, statistical trajectory course corrections were computed during the MDL study and are elaborated on a in a subsequent section.

Table 5: Notional flight validation mission trajectory selected for 2006 CL$_9$.

Property	Value
Earth departure date	2019-08-02
Earth departure C_3	11.99 km^2/s^2
Flight time to intercept NEO	121.41 days
Relative velocity at intercept	11.5 km/s
Approach phase angle	3.04°
Max. distance from Earth	0.36 AU
Max. distance from Sun	1.28 AU

6. Mission Design Lab Results

The objective of the MDL study is primarily to assess the technical feasibility of deploying a spacecraft to intercept a small (50–100 m) NEO within 10 m of its center with 3σ confidence at high relative velocity ($>$ 10 km/s) in order to provide a viable planetary defense solution for short warning time scenarios. The MDL performs this assessment by developing a preliminary spacecraft systems concept for a two-body Hypervelocity Asteroid Intercept Vehicle (HAIV) capable of reliably delivering a notional NED payload to a target NEO and transmitting adequate telemetry for validation of system performance. In addition to the conceptual spacecraft design, the MDL creates associated plans for the supporting mission and ground operations in order to provide an overall mission architecture. The MDL worked to design a fully capable HAIV (rather than a simplified test platform) and apply the fully capable design to a suitable practice target NEO (as described previously in the section about target selection). The MDL endeavored to make the flight validation mission affordable through judicious mission design rather than via a scaled-down less expensive flight demonstration platform.

The primary design drivers are the high relative velocity at impact and the precision timing required for detonation of the NED in the shallow crater excavated by the leading kinetic impactor portion of the vehicle. The MDL carefully considered what systems equipment should be placed on the lead portion (kinetic impactor) of the HAIV and what should be placed on the follower portion (NED payload carrier). Additionally, high reliability is required because there will only be one opportunity to successfully strike the target NEO. These considerations make it clear that the HAIV will need to be a highly responsive system with onboard autonomous control because of the latency inherent in ground commanding and the highly dynamic environment of the terminal approach phase. Yet another challenging aspect of this mission is that the size, shape, and rotational state of the NEO will generally not be known in advance of the intercept mission.

Design, selection, fuzing, and so on for the NED was purposely placed outside the scope of the MDL study. For the purposes of the study we assume that a dummy mass proxy for the NED payload is installed in the HAIV for the flight validation mission. The NED proxy is modeled as a cylinder 1 m in length with a 0.5 m face diameter and a mass of 300 kg.

The overall mechanical design for the HAIV created by the MDL is presented in Figure 9 and shows the leading impactor portion of the vehicle, the trailing follower portion of the vehicle (carrying the dummy mass proxy for the NED), and the 10 m AstroMast extendable boom that provides the necessary separation between the impactor and follower during NEO impact while ensuring that the two parts of the vehicle remain collinear during impact. The length of the boom is customized for the particular mission scenario at hand such that the boom length provides an appropriate delay time between when the impactor creates the crater on the NEO and when the follower arrives in the crater and detonates the NED. The appropriate delay time is of course dependent on the terminal approach profile, which is chiefly dominated by the HAIV velocity relative to the NEO at impact.

11

Figure 10 shows another view of the HAIV with selected dimensions and mass properties labeled, while Figure 11 provides a more detailed view of the follower portion of the HAIV with selected subsystem components labeled.
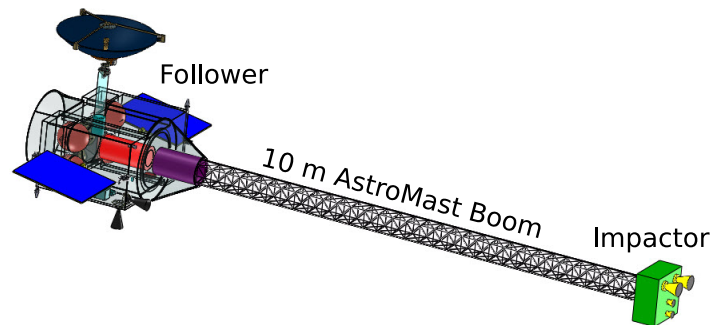

Figure 9: Conceptual HAIV design showing the follower, boom, and impactor vehicle components.
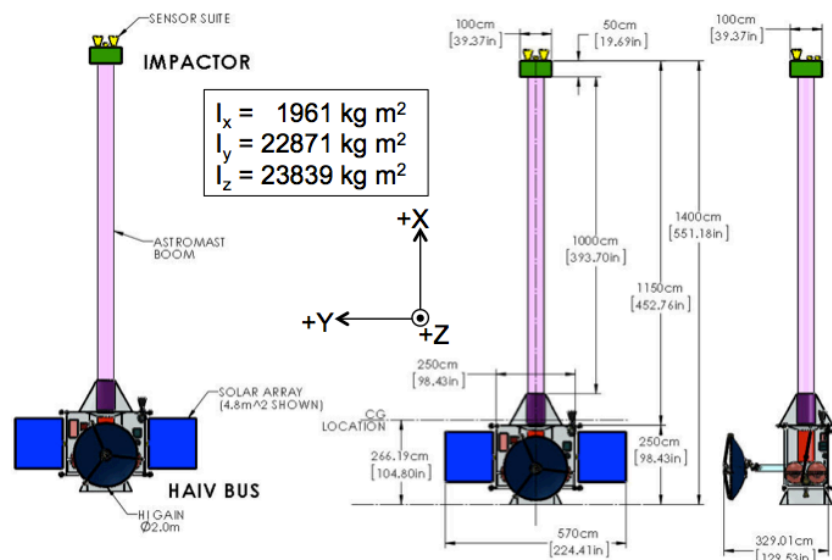

Figure 10: Conceptual HAIV design with dimensions and selected mass properties.

In the following we present a mission overview, detailed descriptions of selected subsystems, the mission cost estimate, and a discussion of key future research topics identified during the MDL study.

6.1. Mission Overview

For launch vehicles, the MDL considered the United Launch Alliance (ULA) Atlas V 400/500 Evolved Expendable Launch Vehicle (EELV) Series, the SpaceX Falcon 9, and the Boeing Delta IV series. All of these launch vehicles provide sufficient mass capability at the desired Earth departure C_3 but the Atlas V is the only EELV currently covered under the NASA Launch Servies Program II contract. As such, the Atlas V 401 with a 4 m fairing was selected as the primary launch vehicle for the MDL study. The HAIV launch configuration in the Atlas V 401 payload fairing is shown in Figure 12. Accordingly, the HAIV will launch from Cape Canaveral Air Force Station (CCAFS).

The basic schedule envisioned for the HAIV flight validation mission project is summarized in Table 6. A project start date of May 1th, 2015 is assumed and the project schedule is developed from that assumed start date. The first phase is preliminary analysis (Phase A, 6 months), which is followed by the definition phase (Phase B, 12 months). The Preliminary Design Review (PDR) occurs at the end of Phase B, and the Critical Design Review (CDR) takes place at the end of the phase that follows, which is the design phase (Phase C, 12 months). The next phase (Phase D, 21.13 months) includes subsystem development, fabrication, spacecraft integration and test, and launch on August 2nd, 2019. Nominal operations and mission closeout (Phase E/F, 5 months) follow launch, with target NEO impact occurring on December 2nd, 2019.
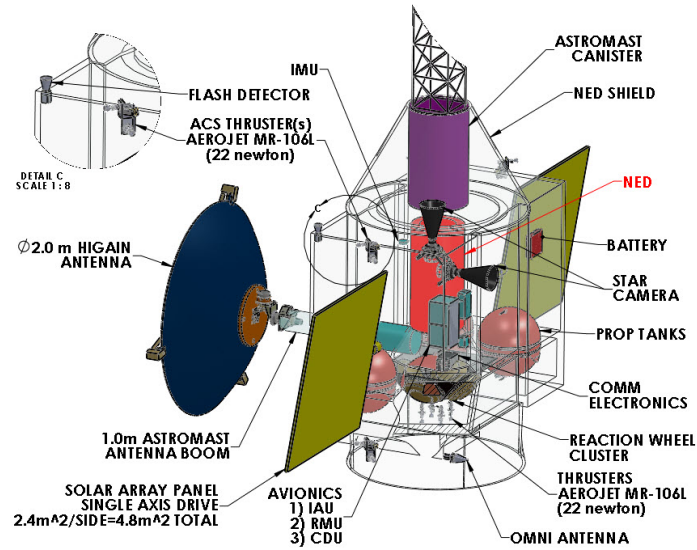
Figure 11: Detail view of the follower portion of the HAIV showing selected subsystem components.
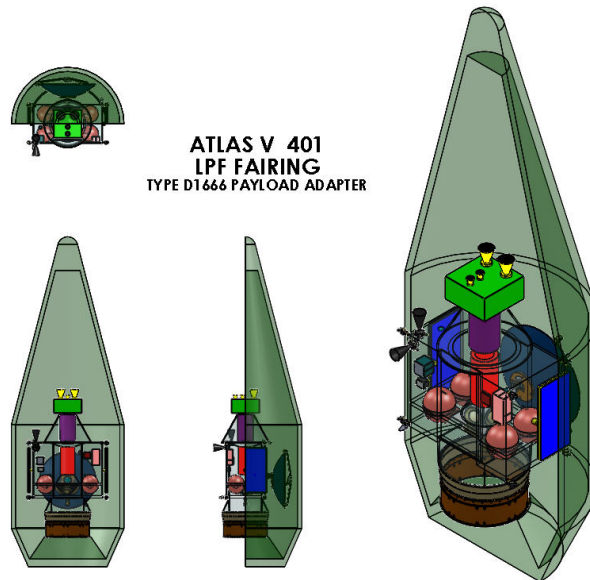

Figure 12: HAIV launch configuration.

Table 6: Project schedule summary.

Period 0	Project Start to End of Phase A	2015-05-01 – 2015-10-31
Period 1	Start of Phase B to End of Phase C	2015-10-31 – 2017-10-30
Period 2	End of Phase C to mid Phase D	2017-10-30 – 2019-06-05
Period 3	Mid Phase D to Launch - 1 month	2019-06-05 – 2019-07-03
Period 4	Launch - 1 month to Start of Nominal Operations	2019-07-03 – 2019-08-17
Period 5	Nominal Operations	2019-08-17 – 2019-12-02
Period 6	Mission Closeout	2019-12-02 – 2020-01-01

Figure 13(a) presents the overall mission timeline, beginning with launch on August 2nd, 2019. Launch is followed by two weeks of on-orbit checkout (during the Earth departure trajectory), which leads into approximately 121 days of outbound cruise towards the target NEO. Although the flight validation mission only carries a simple mass proxy for the NED, we will treat it as if it were a live explosive payload and go through the same steps that

13

we would with the live payload. Thus the payload is "armed" 30 days prior to NEO impact (I - 30 days). The onboard targeting system is engaged at I - 48 hours and images of the NEO (still very small in the camera FOV) begin to be transmitted to the ground. The boom is then extended to deploy the impactor at I - 24 hours.

Figure 13(b) shows the mission timeline for the final 2 hours. At I - 2 hours the ground relinquishes control to the vehicle and the Terminal Guidance Maneuvers (TGMs) begin. At the final 60 seconds before impact the HAIV is 660 km away from the NEO and is transmitting 10 images per second to the ground, with the final image downlinked at I - 1 second. At I - 0 the impactor contacts the surface of the NEO (creating a shallow crater) and that event causes the fire command to be issued to the NED mass proxy (which is instrumented with the same circuitry that would be used with an actual NED). At I + 1 millisecond the follower portion of the vehicle enters the crater and the NED would detonate at this time (due to the fire command having been issued at the proper time 1 millisecond prior to crater entry).

(a) Overall mission timeline.
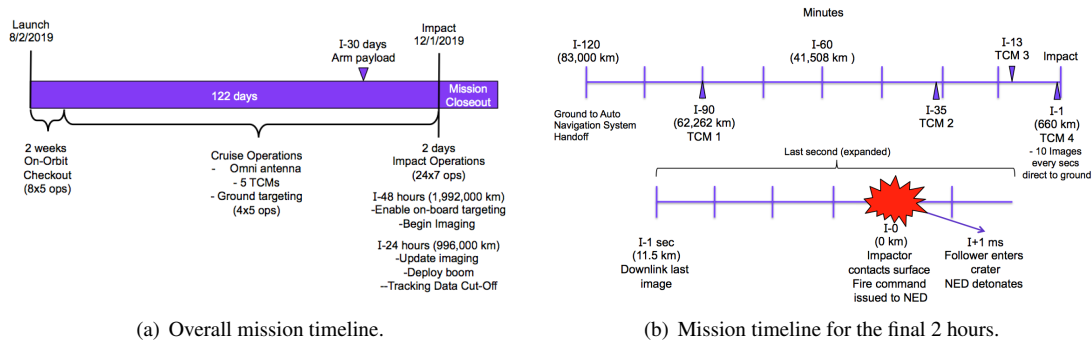
(b) Mission timeline for the final 2 hours.

Figure 13: HAIV flight validation mission timeline.

Table 7 summarizes the performance of the instruments assumed for the HAIV. The NAVCAM provides images centered on the NEO (which only occupies a very small percentage of the FOV until shortly before impact, as will be shown in a subsequent section). These images are used for internal navigation functions onboard the spacecraft and are also transmitted to the ground to provide situational awareness, enable reconstruction of the spacecraft's final approach to impact, and provide pre-impact visible wavelength images of the impact site. The IMPACTCAM collects and transmits imagery of the NEO at a higher frame rate and lower resolution during the final 60 seconds before impact to provide additional situational awareness and facilitate an in-depth reconstruction of the spacecraft's collision with the NEO so that the ground can verify that impact accuracy requirements were met correctly in post-processing. More details about these instruments are provided in subsequent sections. Finally, a hypervelocity contact sensor is utilized to detect the collision of the leading kinetic impactor portion of the vehicle with the NEO, and that collision detection signal is used to send the fire command to the NED proxy payload. Note that communications between the impactor and follower portions of the vehicle are hard-wired (i.e., no radio signals are exchanged between the vehicles).

Table 7: Instrument performance values.

Instrument	Data Rate	Frame Rate	Start Time
NAVCAM (Internal Navigation Frames)	8.4 Mbps	1/min	I - 48 hours
NAVCAM (Image Frames for Transmission to Ground)	400 kbps	5/sec	I - 48 hours
IMPACTCAM	65 kbps	10-17/sec	I - 60 seconds
Contact Sensor	-	-	Triggered by Impact

The detailed mass summary for the HAIV is provided in Table 8 according to the two parts of the HAIV (impactor and follower), their subsystems, and the NED proxy payload. The vehicle design includes the necessary redundancy for a Class A mission, and this is reflected in the mass values shown. The total wet mass of the HAIV launch is computed to be about 1200 kg, including contingencies. However, the Atlas V 401 has approximately twice that mass capability at our Earth departure C_3 of 12 km^2/s^2. That provides a substantial amount of margin for spacecraft mass growth during development leading up to launch. It also means that a smaller (less expensive) launch vehicle could theoretically be utilized for this mission if such a launch vehicle existed. It is important to note that the total propellant mass required for the mission is only 64 kg. The mission Δv and propulsion system

design are detailed in subsequent sections, and those discussions show that the total propellant capacity of the HAIV is about 364 kg. Thus, if the propellant tanks are filled to capacity then the propellant load becomes 363.8 kg. That raises the CBE spacecraft wet mass (launch mass) to 1345 kg (from 1045 kg in Table 8), and with a contingency of 12% the MEV spacecraft wet mass (launch mass) becomes 1500.7 kg. That leaves a launch vehicle throw mass margin of 814 kg (down from 1114 kg in Table 8) or 54.3% (down from 92.8%). The mass margin above 15% becomes 39.3% (down from 77.8%). It is therefore possible to provide the spacecraft with a significant amount of excess Δv capability while maintaing very robust mass margins.

Table 8: Spacecraft mass summary with minimum propellant load.

Payload Mass			
NED	CBE (kg)	Contingency (%)	MEV (kg)
Payload Dry Mass	300.0	0	300.0
Payload Wet Mass	0.0	0	0.0
Total Payload Mass	300.0	0	300.0
Impactor Bus Dry Mass			
	CBE (kg)	Contingency (%)	MEV (kg)
ACS-NAVCAM 1,2 ($\times$ 2)	10.0	0	10.0
ACS-IMPACTCAM 1,2 ($\times$ 2)	2.0	0	2.0
ACS-Impact Sensor	2.0	0	2.0
Mechanical Impactor	136.0	0	136.0
Power (2 Lithium-Ion Battaries, 12.33 kg)	12.3	0	12.3
Spacecraft Bus Dry Mass total	162.3	0	162.3
Follower Bus Dry Mass			
	CBE (kg)	Contingency (%)	MEV (kg)
Attitude Determination and Control	52.7	30	68.4
Mechanical	82.5	30	106.7
AstroMast Boom	38.3	30	49.7
Thermal	32.8	30	42.6
Propulsion	80.3	30	104.4
Power (SA, Battery, Harness, no PSE)	92.9	30	120.7
Avionics	59.2	30	77.0
Communications	80.8	30	105.0
Spacecraft Bus Dry Mass Total	681.2	23	836.8
Total Spacecraft Mass			
	CBE (kg)	Contingency (%)	MEV (kg)
Payload Total	300.0	0	300.0
Spacecraft Bus Dry Mass	681.2	23	836.9
Total Dry Mass	981.2	16	1136.9
Propellant (Hydrazine + Pressurant)	64.0	0	64.0
Spacecraft Wet Mass (Launch Mass)	1045.2	15	1200.9
Launch Vehicle Evaluation			
Launch Vehicle Capability (Atlas V 401) (kg)			2315
Launch Vehicle Throw Mass Margin (kg)			1114
Launch Vehicle Throw Mass Margin (%)			92.8
Margin Above 15%			77.8

6.2. NED Shielding

One area of concern in the vehicle design is that the follower carrying the NED payload will be flying through the environment created by the collision of the leading kinetic impactor portion of the vehicle. That will certainly

be an extremely energetic environment and the follower portion of the vehicle must therefore have adequate shielding built into it around the NED payload to ensure the integrity of the NED during those crucial final fractions of a second before detonation. The debris analysis performed by the MDL therefore focused on the ejecta and thermal effects that might be produced by the kinetic impact ahead of the follower.

The MDL debris analysis assumes that most of the kinetic energy generated by the impactor collision is consumed in the vaporization of the cavity walls and less energy is used in asteroid fragmentation [7]. Asteroid particles reaching the follower spacecraft are therefore generally considered to be dust-size grains ranging in size from 1 μm to 100 μm (0.1 mm). For the purposes of this analysis, the particles are modeled as granite (density of 2.7 g/cm^3). The maximum particle size is compared with the particle critical diameter, which is the minimum particle diameter capable of perforating the two honeycomb panel cones around the front of the NED housing the follower, shown in Figure 14.
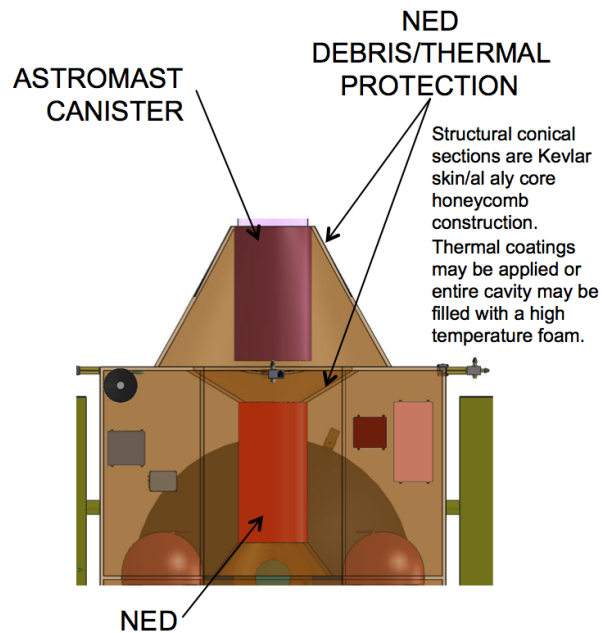

Figure 14: Configuration of NED shielding to protect against debris and thermal effects of kinetic impact.

The Kevlar honeycomb panels provide thermal protection in addition to hypervelocity impact protection and the thickness of the the honeycomb panels can be increased if needed. Protection of the payload from heat generated by impactor collision can be improved by the use of additional materials. The current spaceecraft bus configuration for the follower provides empty space that can be used to implement different shield configurations. Some of the potential methods to increase thermal protection are Spray-On Foam Insulation (SOFI), Phenolic Impregnated Carbon Ablative (PICA), or a solid metallic plate made of aluminum, beryllium, or other material.

The Kevlar honeycomb panels should provide the NED payload with adequate protection from asteroid fragments. With a thickness of 1 mm for each facesheet, the minimum asteroid debris size capable of perforating both Kevlar cones is 5.7 mm in diameter. If future asteroid debris cloud simulations determine that larger particles can be created, then the thickness of the facesheets can simply be increased. A more detailed model for asteroid debris flux that sheds light on the diameter, quantity, and travel directions of particles will be developed in ongoing work.

6.3. Flight Dynamics

As described previously, the launch vehicle selected by the MDL for the conceptual flight validation mission is the Atlas V 401. The 3σ dispersion on the Earth departure C_3 is 0.15 km^2/s^2, which leads to a Δv for launch dispersion correction of approximately 26 m/s, including maneuver execution errors. The Declination of the Launch Asymptote (DLA) and Right ascension of the Launch Asymptote (RLA) are 52.4° and −12°, respectively. The time of injection into the outbound Earth departure hyperbola is 2019-08-02, 08:47:26.443 UTC. The flight time to NEO intercept is 121.41 days, which leads to a time of intercept of 2019-12-01, 18:37:50.443 UTC. The velocity relative to the target at intercept is 11.5 km/s and the approach phase angle is 3°. The maximum distance from the Earth is 0.36 AU and the maximum distance from the Sun is 1.28 AU. This particular trajectory design was assumed to be the middle of the launch window. The conditions associated with the opening and closing of

the mission launch window were computed and are summarized in Table 9. The baseline trajectory solution for the middle of the launch window is plotted in Figure 15.

The total post-launch Δv budget for the mission is 37.1 m/s, detailed in Table 10. In Table 10 TCM stands for Trajectory Correction Maneuver, TGM stands for Terminal Guidance Maneuver, L stands for Launch, and I stands for Impact. The development of the TGM portion of the budget is based on specialized terminal guidance analysis that is presented subsequently.

Table 9: Preliminary launch window.

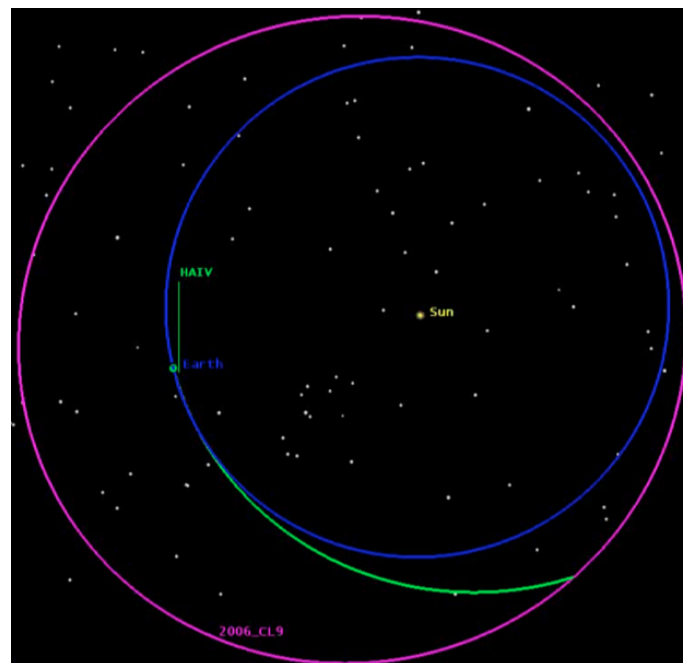|	Open	Middle	Close
Launch date	2019-07-21	2019-08-02	2019-08-12
Earth departure C_3 (km^2/s^2)	22.48	11.99	8.44
RLA	58.6°	52.4°	38.9°
DLA	−3.1°	−12.0°	−20.8°
Relative velocity at intercept (km/s)	13.4	11.5	10.0

Figure 15: Ecliptic plane projection of the Earth's orbit (blue), the orbit of 2006 CL$_9$ (violet), and the HAIV intercept trajectory (green).

6.4. Navigation and Terminal Guidance

The MDL performed a complete navigation simulation of the terminal approach phase beginning at I - 2 hours. The navigation simulation included a linear covariance analysis and a Monte Carlo error analysis. The navigation simulation utilized a sequential Kalman filter with observations derived from the asteroid centroid location in the sensor CCD (Charge-Coupled Device). The navigation filter is solving for the inertial position and velocity of the spacecraft with respect to the asteroid. The simulation software utilized is the Orbit Determination Toolbox (ODTBX)[13].

---

[13]ODTBX is an advanced mission simulation and analysis tool used for concept exploration, proposals, early design phases, and rapid design center environments. ODTBX is developed by the Navigation and Mission Design Branch at NASA Goddard Space Flight Center. The software is released publicly under the NASA Open Source Agreement and is available on SourceForge at `http://sourceforge.net/projects/odtbx/`.

Table 10: Maneuver schedule and Δv budget.

Maneuver	Δv (m/s)	Time	Correction	Δv Error (%)	Δv Error (m/s)
TCM 1	26.0	L + 01 days	Launch vehicle insertion (3σ)	10	2.6
TCM 2	2.8	L + 10 days	TCM 1 error	5	0.140
TCM 3	0.3	L + 30 days	TCM 2 error	5	0.015
TCM 4	0.2	L + 60 days	TCM 3 error	5	0.010
TCM 5	0.3	L + 90 days	TCM 4 error	0	0.000
TGM 1	3.1	I - 90 min	Nav and TCM 5 error	-	-
TGM 2	0.4	I - 35 min	Nav and TGM 1 error	-	-
TGM 3	0.5	I - 13 min	Nav and TGM 2 error	-	-
TGM 4	3.5	I - 60 secs	Nav and TGM 3 error	-	-
Total Δv	37.1				

The optical navigation sensors modeled in the simulations are based on the Deep Impact mission's Impactor Targeting Sensor (ITS), which has a Field Of View (FOV) of 0.6°, a focal length of 2101 mm, and a resolution of 1024×1024. The navigation relies on identification of the target body centroid in the sensor field of view. The acquistion requirement is to be able to detect a 13th apparent magnitude object with a signal-to-noise ratio of at least 10 within a 5 second exposure.

(a) Optical acquisition time for low and high NEO albedo.
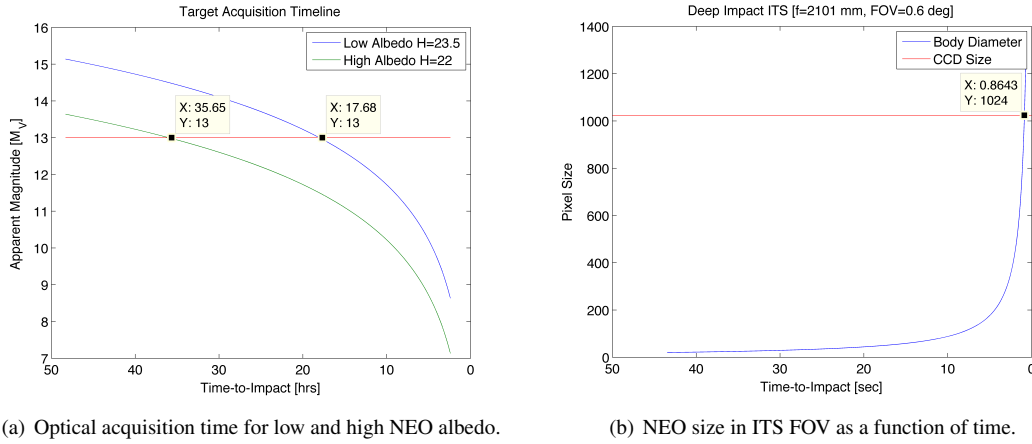
(b) NEO size in ITS FOV as a function of time.

Figure 16: Timelines for NEO acquisition and size in ITS FOV.

Figure 16(a) shows when the ITS is able to acquire the target NEO in terms of time until impact for the high (0.25) and low (0.13) albedo cases defined for this study. The effect of NEO albedo is quite clear: acquisition occurs at I - 35.65 hours for the high albedo case and only I - 17.68 hours for the low albedo case. If the NEO's albedo turns out to be < 0.13, it could be problematic for the terminal guidance sequence due to acquisiton occurring too late prior to impact. This problem is being studied further in ongoing research. Figure 16(b) shows the size of the NEO in the ITS FOV as a function time before impact. The high intercept velocity and the NEO's small size mean that the NEO will not even begin to fill the FOV until a few seconds before impact.

The error sources modeled in the navigation simulation include spacecraft a priori state uncertainties of 5 km in position and 1 cm/s in velocity, 3-axis spacecraft attitude uncertainty of 10 μrad, random centroid pixel noise of 0.05 pixels with a 0.1 pixel bias, and proportional and fixed maneuver execution errors of 1% and 1 mm/s, respectively. All of these error values are 1σ.

Figure 17 presents a block diagram for the Autonomous Navigation System (ANS) that is modeled in simulation to perform navigation and compute Terminal Guidance Maneuvers (TGMs). TGM targeting is based on the latest estimate of spacecraft state from the Kalman filter, which encapsulates both navigation and maneuver execution errors. Four TGMs are performed after optical acquisiton to correction for navigation and execution errors. TGMs 1 through 3 are targeted using full three-dimensional differential correction while TGM 4 is targeted using two-dimensional B-plane targeting. This was found to be the most robust targeting scheme after initial experimen-

tation because the range between the HAIV and the NEO is not very observable and that compromises targeting schemes that rely solely on full three-dimensional position targeting. The ground-to-ANS handoff occurs at I - 2 hours, at which time the flight dynamics system on the ground provides a final state update to the HAIV and hands over translational control to the ANS. The ANS computes and executes TGMs at I - 90 minutes, I - 35 minutes, I - 12 minutes, and I - 1 minute.
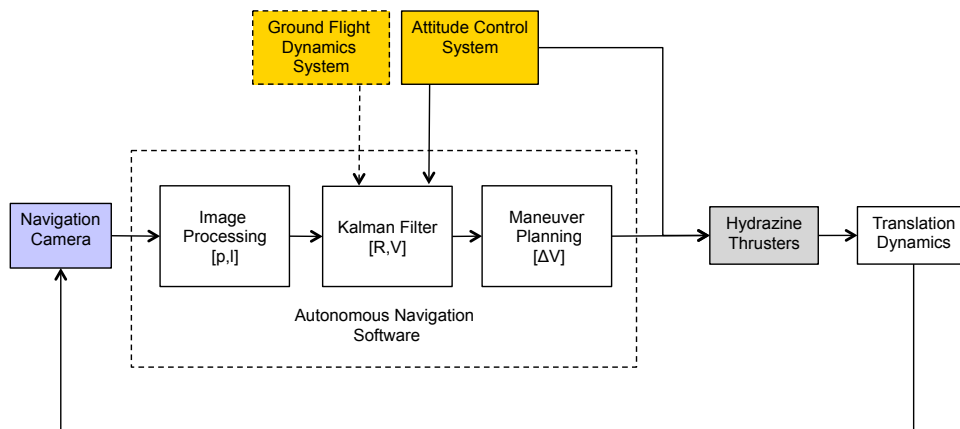

Figure 17: Block diagram of the Autonomous Navigation System (ANS) modeled in simulation.

The ANS was exercised for our target NEO scenario with a Monte Carlo simulation to characterize performance in terms of impact accuracy. Due to study time constraints only 100 Monte Carlo cases were executed to produce the preliminary results shown herein. Figure 18(a) shows the impact locations in the B-plane while Figure 18(b) shows the corresponding impact locations on the body of the target NEO. Note that the area of brightness on the surface of the spherical NEO model shown in Figure 18(b) accurately depicts the solar illumination in the associated mission scenario.
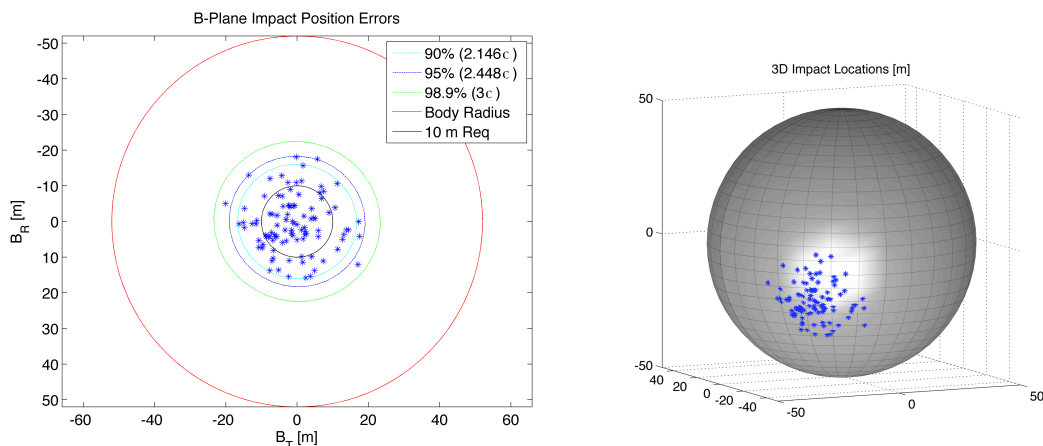
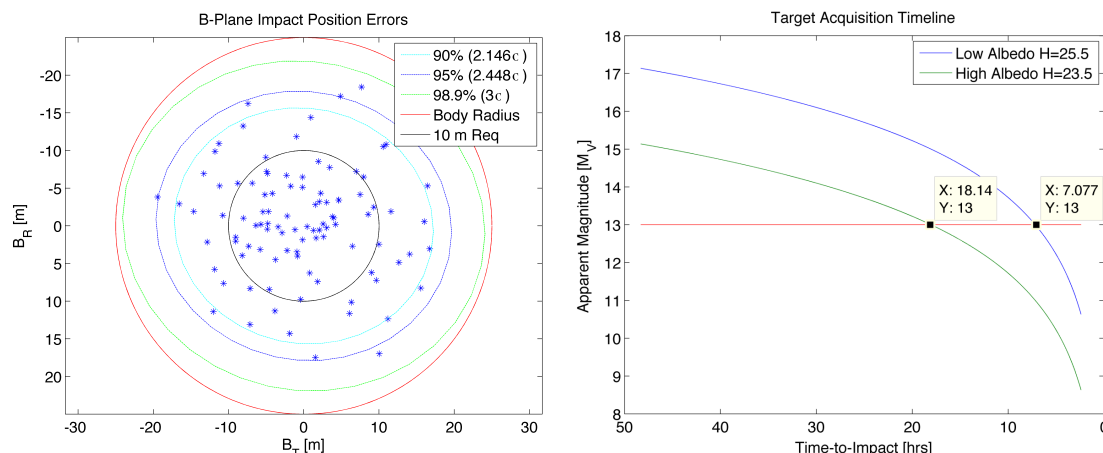(a) Simulated HAIV impact locations in the B-plane.
(b) Simulated HAIV impact locations on the target NEO body.

Figure 18: Simulated HAIV impact locations on the target NEO from a Monte Carlo simulation.

The major axes of the 90%, 95%, and 98.9% impact location error ellipses (which correspond to 2.146σ, 2.448σ, and 3σ confidences, respectively) are 16.77 m, 19.13 m, and 23.44 m, respectively. Overall, 56% of the 100 cases meet the 10 m requirement. While those results do not satisfy the impact accuracy requirement of 10 m with 3σ confidence, the impact locations are clearly well-clustered about the center of the NEO and we are working to tune the ANS in ongoing research to meet our accuracy requirement.

A second Monte Carlo analysis using the same simulation parameters described above was performed for a 50 m size NEO to address one of our MDL study goals, which is to assess the feasibility of accurately and reliably intercepting a NEO as small as 50 m at hypervelocity. The impact location errors are shown in Figure 19(a). In this case the major axes of the 90%, 95%, and 98.9% impact location error ellipses are 17.31 m, 19.74 m, and 24.20 m, respectively. Those values are comparable to the values achieved in the 100 m NEO analysis, but the

impact location spread relative to the NEO's surface is much larger for the smaller NEO, as seen in Figure 19(a). Another aspect of a 50 m target NEO is that its smaller size will delay optical acquisition compared to the 100 m NEO case, all else being equal. As shown in Figure 19(b), optical acquisition of the 50 m NEO does not occur until I - 18.4 hours for the high albedo case and I - 7.08 hours for the low albedo case. Thus, for a given approach velocity, later acquisitions will require faster ground processing. In some cases it may be possible to re-target the outbound cruise trajectory (from Earth to the NEO) to reduce the approach velocity somewhat, but only to the extent that the crater created by the lead portion of the HAIV still meets mission requirements.

(a) Simulated HAIV impact locations in the B-plane for a 50 m NEO.

(b) Optical acquisition time for low and high albedo for a 50 m NEO.

Figure 19: Timeline for acquisition of a 50 m target NEO and impact accuracy results from a Monte Carlo simulation.

The statistical results for the TGMs for the 100 m NEO analysis are summarized in Table 11. These values informed the construction of the mission Δv budget presented in Table 10.

Table 11: Terminal Guidance Maneuver (TGM) statistics.

Maneuver	Minimum (m/s)	Maximum (m/s)	Mean (m/s)	Mean + 3σ (m/s)
TGM 1 Δv	0.1557	2.9892	1.1705	3.0643
TGM 2 Δv	0.0127	0.4065	0.1451	0.3807
TGM 3 Δv	0.0120	0.5006	0.1812	0.4790
TGM 4 Δv	0.1689	3.4926	1.3377	3.5045
Total	-	-	2.8345	7.4285

6.5. Attitude Control System

The HAIV Attitude Control System (ACS) is designed to provide stable pointing throughout all mission phases from launch to NEO impact. After launch the ACS will null residual tip-off motion and acquire the appropriate mission attitude, with the solar arrays pointing to the Sun. During outbound cruise, up until the terminal approach phase begins, the ACS will facilitate solar array pointing to the Sun (the arrays are able to rotate completely about the $+Y$ spacecraft body axis). The ACS will also facilitate pointing of the high-gain antenna to the Earth with a pointing accuracy of $0.1°$. The antenna can be slewed in two axes over a restricted angular range. The ACS will also keep the cold side of the spacecraft pointed away from the Sun for appropriate thermal control. For maneuvers the ACS will point the thruster centerlines within $0.5°$ of the designated inertial coordinates. During the terminal approach phase the ACS will nominally hold the $+X$ spacecraft body axis parallel to the spacecraft's velocity vector. That pointing will be maintained by using thrusters to translate transversely. Additionally, the star camera may be provided as a backup to the impact sensors.

The ACS for this mission requires a relatively straightforward three-axis stabilized system, and the ACS system components are listed in Table 12. The attitude sensors include two star cameras and an inertial reference unit

(gyros and possibly an accelerometer package). While two camera heads are baselined in the design, the data processing unit can accommodate up to four camera heads if needed. The attitude actuators include four reaction wheels arranged in a pyramid to provide mutual redundancy along with hydrazine thrusters. The following attitude control modes are defined for this mission: acquisition, cruise, ΔV, ΔH, terminal phase, and safehold. The ACS will be operating continuously using the reaction wheels, and the attitude control thrusters will be used at discrete times for momentum unloading. The attitude control thrusters may also be needed during any "turn-and-burn" maneuvers. During the terminal phase, when the ANS is initialized the ACS software will provide the inertial-to-body frame quaternion to the ANS.
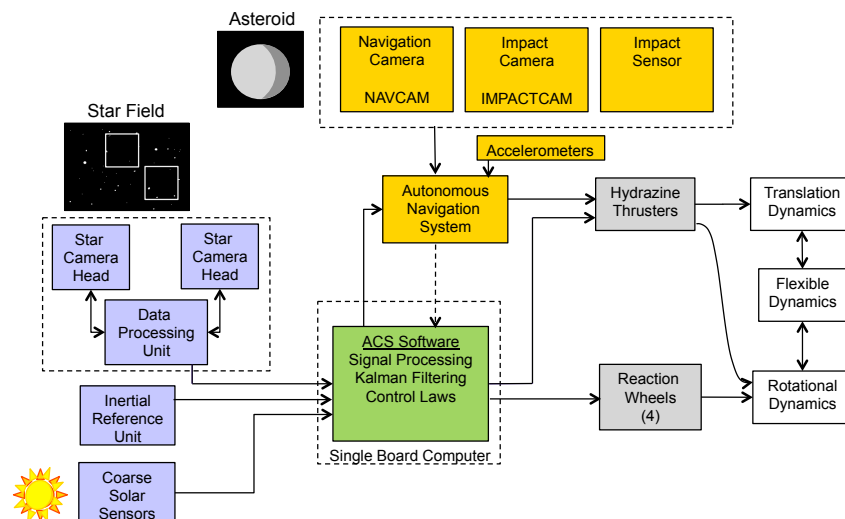

Figure 20: Attitude control system block diagram.

Table 12: Attitude control system components.

Components	Vendor	Model	Quantity	Total Mass (kg)	Total Avg. Power (W)
IMU	Northrop Grumman	SIRU	1	3.18	20.0
Star Camera	Oersted	Advanced Stellar Compass			
		Camera Heads	2	0.50	1.2
		Data Processing Units	1	0.91	7.0
Coarse Sun Sensors	Adcole	Coarse Solar Sensors	12	0.06	1.2
Reaction Wheels	Honeywell	HR16 (50)	4	48.00	32.0
Total	-	-	-	52.65	58.9

6.6. Propulsion

The propulsion system type selected for the HAIV by the MDL is monopropellant hydrazine operating in a blow-down mode from 400 to 100 psi. The system consists of four propellant tanks and twelve 22 N thrusters. The propulsion system is designed to provide Δv and 3-axis attitude control from launch vehicle separation until impact. Δv is available along all the $+X$, $\pm Y$, and $\pm Z$ axes, and the thruster system supports momentum unloading. The propulsion system is designed to be single-fault tolerant. The three-axis attitude control is provided by eight of the thrusters that are canted at $45°$ and coupled moments are produced by four of the thrusters. The total thrust capability along the X, Y, and Z directions is 88 N, 31-62 N, and 31-62 N, respectively. For Δv maneuvers in the X direction there are four thrusters firing continuously with off-pulsing for control. For Δv in the lateral (Y & Z) directions, two thrusters are fired continuously while pulsing two thrusters.

A monopropellant system was selected in favor of a bipropellant system despite the latter's higher efficiency (specific impulse). The rationale for this choice is that the monopropellant diaphragm tanks manage slosh and prevent gas ingestion during lateral burns whereas the bipropellant tanks are susceptible to gas ingestion. Additionally, the monopropellant system is simpler, more reliable, and less expensive, all else being equal.

The thruster ensemble consists of twelve Aerojet MR-106L 22 N thrusters. Each of the four diaphragm tanks is an ATK 80323-1 23×25 inch 6Al-4V titanium tab mount tank with a mass of 14.3 kg and a maximum operating

pressure of 550 psi. Altogether these four tanks provide a propellant capacity of 360 kg in blow-down mode. All of the components are Commercial Off-The-Shelf (COTS) components. Engineering maneuvers will be performed prior to the terminal phase to characterize thruster performance before terminal maneuvers are executed. The propellant budget is summarized in Table 13 and we note that while the tanks provide a propellant capacity of 360 kg, the current mission design only requires 64 kg of propellant. This provides significant margin for other maneuvering that may be required during the mission due to contingencies. We also note that the burn time for the final TGM is longer than 1 minute, but the final TGM is performed at I - 1 minute. In ongoing work we are therefore trading several design options including increased thrust levels, the timing of the final TGM, and GNC algorithm design strategies that provide sufficient accuracy but purposely keep the final TGM small.

Table 13: Propellant mass budget.

Maneuver	Δv (m/s)	ACS Tax	Effective Δv (m/s)	Effective I_{sp} (s)	HAIV Mass (kg)	Propellant Mass (kg)	Burn Time (s)
Checkout/Engineering Burns	2.3	0	2.30	229	2310.0	2.4	60.4
LV Dispersion, L + 1 day	26.0	50	39.00	229	2307.6	39.8	1014.2
Correction 2, L + 10 days	2.8	50	4.20	229	2267.9	4.2	108.2
Correction 3, L + 30 days	0.3	50	0.45	162	2263.6	0.6	32.1
Correction 4, L + 60 days	0.2	50	0.30	162	2263.0	0.4	21.4
Correction 5, L + 90 days	0.3	50	0.45	162	2262.6	0.6	32.1
TGM 1, I - 90 minutes	3.1	50	4.65	162	2261.9	6.6	330.8
TGM 2, I - 35 minutes	0.4	50	0.60	162	2255.3	0.9	42.6
TGM 3, I - 12 minutes	0.5	50	0.75	162	2254.5	1.1	53.2
TGM 4, I - 1 minutes	3.5	50	5.25	162	2256.4	7.4	372.0
Totals	39.4	-	57.95	-	2246.0 (final)	64.0	2066.8

6.7. Communications

The HAIV must transmit telemetry continuously during final approach and impact because we assume that no observer spacecraft is present near the NEO. Accordingly, the trajectory design must ensure uninterrupted communication with the Deep Space Network (DSN) during the terminal approach phase, which covers the final 24 hours of the mission. Furthermore, the telemetry must be at a sufficiently high rate to downlink real-time image data from the cameras. The telemetry transmission only ends when the HAIV is destroyed at the time of impact. Furthermore, the telemetry stream must contain sufficient data to verify that mission goals are satisfied via telemetry post-processing on the ground. A telemetry Bit Error Rate (BER) of 10^{-6} is assumed for the image data.

Spacecraft navigation via DSN will be important so that the spacecraft state is known well enough to enter the terminal phase with sufficiently accurate state knowledge. Accordingly, we assume DSN tracking for 30 minutes per day throughout the 121 day cruise to the asteroid. There are > 15 minute gaps in DSN coverage during the first 90 days of the outbound cruise. Housekeeping (4 kbps) and image data are downlinked in real-time.

The communications system includes dual X-Band transponders, which support ranging and two-way Doppler with DSN. The DSN can also provide Delta-Differential One-way Ranging (Delta-DOR). The HAIV also has a 2 m High-Gain Antenna (HGA) and an X-Band omni antenna. The HGA will have dual gimbals and requires spacecraft pointing to within ± 0.3° for X-Band. The HGA is sized such that it is the largest antenna that can be accommodated by the launch vehicle fairing. The X-Band omni antenna is used for inital checkout after launch, commanding, telemetry, and ranging. They can provide very low rate telemetry, commanding, and ranging out to 0.36 AU. One hemi antenna is placed on each side of the spacecraft bus and the cross dipole yields -4 dB worst case hemispherical coverage (excluding interference from other omni). Low Density Parity Check (LDPC) of 1/2 is used for efficient, accurate commanding. Convolutional encoding rate of 1/2 is used for quick telemetry. 200 bps X-Band commanding is possible through the omni, even at 0.36 AU. The data storage for the communications system will be at least 0.5 GB, and that is mostly for buffering. The peak DC communications power is 237.7 W and the total mass of the communications equipment is 80.8 kg.

6.8. Power

The HAIV is equipped with two 2.08 m^2 solar arrays, each of which has a single-axis roll drive. The arrays are triple-junction Gallium Arsenide operating at 29.5% efficiency, and the MDL assumes a solar constant of 791 W/m^2. Three extra strings were added to the arrays for fault tolerance and reliability, yielding a total of 27 strings. Two secondary rechargeable Lithium-Ion 20 amp-hour batteries are installed in the follower portion of the HAIV

(one is primary, the other is a backup). Each of those batteries contains eight cells with bypass switches (system can operate on seven or eight). Battery Depth Of Discharge (DOD) will be 3.8% at launch. The battery provides a contingency option during final approach to NEO impact in case the solar arrays are unexpectedly damaged. The 13 primary batteries (not rechargeable) are used in the impactor portion of the HAIV to avoid power cable stiffness in the boom and to provide increased reliability and fault tolerance redundancy. Overall, the 4.16 m^2 solar array area supports the spacecraft power consumption level of 705.3 W with margin; the end-of-life solar array power generated is 842 W.

6.9. Cost Estimate

The estimated cost of this mission is \$530.4M, including the launch vehicle[14]. The cost estimate is comprehensive and includes the complete design, construction, integration, and testing of the spacecraft itself, launch vehicle integration and test, project management, mission operations, ground system, systems integration and test, education and public outreach, and project reserves.

6.10. Key future research topics

Technologies and algorithms must be developed and and validated to create sensors capable of accurately and reliably detecting the hypervelocity collision of the impactor with the NEO. These sensors could be hypervelocity electromechanical contact sensors, some form of LIDAR or radar, a visible flash detector, or some other type of device. The number of sensors and the manner of their operation must be such that robust hypervelocity impact detection is provided, i.e., false positives and false negatives must both be prevented with adequate confidence. The appropriate number of sensors will be informed by the type of sensors used, and reliability is a key factor. For example, with 3 sensors providing impact detection signals (to be used as the NED fire command) and the signals being OR'ed, the reliability of each signal would need to be better than 95%. Addtional sensors and/or multiple sensor types may be necessary if an adequate confidence of successful fire commanding cannot be provided with a given set of sensors. The design of the hypervelocity impact sensors will be informed by rigorous high-fidelity computational modeling of the hypervelocity kinetic impact event, and ground validation of some candidate sensor types may be possible, e.g., using hypervelocity impact facilities in terrestrial laboratories. Such ground test campaigns could utilize scale models of the HAIV instrumented with candidate impact detection sensors. Another aspect of the design that would benefit tremendously from ground testing is the NED shield. The behavior of the boom during the hypervelocity impact is another key area that must be studied through both high-fidelity computer simulations and possibly ground testing. We must be certain that the size, shape, and materials used to construct the boom fail during the hypervelocity impact in a manner that does not threaten the NED payload, the impact sensors, or the production and reception of the NED fire command signal. This raises the possibility of another trade study that we are considering, the purpose of which is assess the feasibility, advantages, and disadvantages of having the impactor and follower be physically separated free-flying vehicles rather than connected by a boom.

Another key area of analysis is the final approach timeline. Our results presented herein demonstrate that the final approach timeline depends on the target NEO diameter and albedo, as well as the approach phase angle relative to the NEO and the relative velocity at impact. Developing parametric models for the approach timeline as a function of these and other key driving parameters will facilitate refinement of the onboard optical systems to ensure acquisiton of the target sufficiently far in advance of the impact for the ANS to be able to operate robustly and achieve a precise and accurate impact with high confidence. We can also adjust our trajectory optimization algorithms to attempt to minimize the intercept velocity within the constraints that the crater excavated on the NEO is of sufficient depth and that the additional maneuver required for intercept velocity control is within our available Δv budget.

One of the driving requirements of the HAIV system is the requirement that the flight experiment must be able to be fully validated in ground post-processing of the HAIV telemetry. While this requirement actually leads to a robust design, it would clearly be beneficial to have an observer spacecraft present near the target NEO before and after the impact to more directly observe and characterize the HAIV performance. As such we have already developed new algorithms to perform trajectory scans that identify mission opportunities in which an observer and HAIV spacecraft can be both transported to the NEO (at different times) for low Δv. The results of these new mission opportunity searches may reveal affordable options for having both an observer and a HAIV in the mission simultaneously. Another alternative worth considering is having the HAIV deploy a free-flying observer that could also serve as calibration target during the cruise to the NEO. The difficulty with this option is that the deployed free-flying system would need to be capable of high bandwidth communications with Earth and would therefore probably be so large that the it cannot reasonably treated as a small deployable add-on; in that case we

---

[14]An approximate cost of \$150M is assumed for the notional launch vehicle, which is the Atlas V 401

return to the aforementioned alternative of deploying a fully capable observer as a separate spacecraft. The final variation on this option is to have another entity supply the observer spacecraft since it is fully decoupled from the HAIV. For example, NASA could build, deploy, and operate the HAIV, while another agency, e.g., ESA, could build, deploy, and operate the observer spacecraft.

Finally, the results presented herein clearly demonstrate that further work is required to improve the performance and robustness of the ANS, particularly in terms of the terminal GNC algorithms. The accuracy must be improved so that statistical impact locations on the NEO surface are always tightly clustered about the NEO center, and the algorithms must be structured to minimize the magnitude of the last TGM or two such that achieving them is well within the capability of the propulsion system (e.g., the accelerations requested by the GNC system are readily achieveable given the spacecraft mass and available thrust). The GNC algorithms will also be upgraded to process synthetic imagery for realistic cases including irregularly shaped rotating NEOs of various sizes to demonstrate that the GNC system is robust to a wide variance in NEO properties. This robustness is important because we will generally not have much information on the physical properties of the NEO before the HAIV is deployed during an actual mission scenario. Accordingly, we are also assessing the effects of NEO density (which will not generally be known in advance) on the cratering performance of the kinetic impactor portion of the HAIV in order to ensure sufficient crater depth for the NED detonation.

7. Conclusions

Earth has been struck by asteroids and comets in the past and will continue to be struck now and in the future. Our geological records, historical records, and observations of recent and upcoming events provide us with ample evidence that the threat of Earth impact by hazardous NEOs is quite real. Although we have sent a number of scientific missions to NEOs, we have never before performed actual flight demonstrations of the planetary defense technologies that we will need to rely upon during a true emergency situation. The goal of our Phase 2 NIAC research project is to design a feasible, effective, and reliable Hypervelocity Asteroid Intercept Vehicle (HAIV) for planetary defense and also design the flight validation mission during which its effectiveness and reliability will be demonstrated. The HAIV is a two-body spacecraft consisting of a lead kinetic impactor portion that excavates a shallow crater on the target into which the follower portion of the spacecraft delivers a Nuclear Explosive Device (NED) and detonates it to perform a subsurface detonation that is approximately 20 times more effective at disrupting the NEO than a surface or standoff detonation. The ability to carry out that sequence at intercept velocities in the hypervelocity regime (> 5 km/s, sometimes > 10 km/s or more), combined with the high efficiency of subsurface detonations, makes the HAIV a highly responsive planetary defense platform for a wide range of hazardous NEO scenarios. In particular, the HAIV provides a viable planetary defense solution for short warning scenarios involving small but dangerous NEOs in the 50 to 100 m size category.

In this paper we have provided background on the threat NEOs pose to Earth, an overview of the NEO missions that have been performed to date and why they do not constitute planetary defense technology demonstrations, a description of the HAIV concept, and the results of a recent NASA/Goddard Space Flight Center (GSFC) Mission Design Lab (MDL) study for the conceptual design of the HAIV flight validation mission in collaboration with the Asteroid Deflection Research Center (ADRC) of Iowa State University as part of the Phase 2 NIAC project research.

The MDL study has provided a feasible and detailed conceptual design for the HAIV flight validation mission and identified a number of key topics for further research that are being pursued by the ADRC and GSFC as part of the ongoing Phase 2 NIAC work. These research topics include high-fidelity computational modeling of hypervelocity impact physics, detailed development of advanced GNC algorithms for precision hypervelocity intercept of small (50–100 m size) NEOs, and design and development of test plans for robust hypervelocity impact sensors. In our ongoing research we will continue to refine, deepen, expand, and advance the design of the HAIV system and its flight validation mission.

When a hazardous NEO on a collision course with Earth is discovered we will not have the luxury of designing, testing, and refining our systems and plans. We will need to be prepared to take effective action on relatively short notice with a high probability of succeeding on the first try because we may not have a second chance. That level of adeptness and preparedness can only be achieved through proper design and testing of systems so that we are comfortable with carrying out planetary defense test and practice missions before we need to deploy such a mission in response to an actual threat.

References

[1] Wie, B., Pitz, A., Kaplinger, B., Hawkins, M., Wagner, S., Vardaxis, G., Winkler, T., and Lyzhoft, J., Optimal Fragmentation and Dispersion of Hazardous Near-Earth Objects, NIAC Phase I Final Report, Grant Number NNX11AR43G, Asteroid Deflection Research Center, Department of Aerospace Engineering, Iowa State University, Ames, IA, 2012.

[2] Vardaxis, G., Pitz, A., and Wie, B., Conceptual Design and Analysis of Planetary Defense Technology (PDT) Demonstration Missions, in: Advances in the Astronautical Sciences, volume 143, Univelt, Inc., San Diego, CA, 2012. Paper number AAS 12-128.

[3] Pitz, A., Kaplinger, B., Vardaxis, G., Winkler, T., and Wie, B., Conceptual Design of a Hypervelocity Asteroid Intercept Vehicle (HAIV) and Its Flight Validation Mission, in: Proceedings of the 2012 IAF/AIAA Global Space Exploration Conference, Washington, DC. May 22-24, 2012. Paper number GLEX-2012.06.312173.

[4] Winkler, T., Wagner, S., and Wie, B., Optimal Target Selection for a Planetary Defense Technology (PDT) Demonstration Mission, in: Advances in the Astronautical Sciences, volume 143, Univelt, Inc., San Diego, CA, 2012. Paper number AAS 12-226.

[5] Wagner, S., Winkler, T., and Wie, B., Analysis and Selection of Optimal Targets for a Planetary Defense Technology Demonstration Mission, in: Proceedings of the 2012 AIAA/AAS Astrodynamics Specialist Conference, Minneapolis, MN. August 13-16, 2012. AIAA Paper Number 2012-4874.

[6] Barbee, B. W., Mink, R. G., Adamo, D. R., and Alberding, C. M., Methodology and Results of the Near-Earth Object (NEO) Human Space Flight (HSF) Accessible Targets Study (NHATS), in: Advances in the Astronautical Sciences, volume 142, Univelt, Inc., San Diego, CA, 2011, pp. 613–632.

[7] Kadono, T., Hypervelocity impact into low density material and cometary outburst, Planetary and Space Science 47 (1999) 305–318.